LA-UR-96- 899

Title:

Laser-Ultrasonic Evaluation of Damage in Unidirectional Ceramic Matrix Composites

Author(s):

Yongmei Liu, CMS
Terence E. Mitchell, CMS
Haydn N. G. Wadley, University of Virginia

Submitted to:

Poster will be presented at
98th Annual Meeting of American Ceramic Society
Indianapolis, IN
April 14-17, 1996

Los Alamos
NATIONAL LABORATORY

LASER-ULTRASONIC EVALUATION OF DAMAGE IN UNIDIRECTIONAL CERAMIC MATRIX COMPOSITES

Y.-M. Liu, T. E. Mitchell, Center for Materials Science, Mail Stop K765
Los Alamos National Laboratory, Los Alamos, NM 87545, U. S. A.
and H. N. G. Wadley, Department of Materials Science and Engineering, School of Engineering and Applied Science, University of Virginia, Charlottesville, VA 22903, U. S. A.

INTRODUCTION

Ceramic matrix composites (CMCs) have attracted great attention because of their potential for high temperature structural applications. Among these materials, calcium aluminosilicate (CAS) glass ceramic and similar composites reinforced by Nicalon™ SiC fiber with carbon-rich interface have been under active investigation because of their "notch-insensitivity": stress near holes and notches can be redistributed by inelastic deformation in the form of multiple matrix cracking [1-3]. Therefore, stress concentration is alleviated near these sites.

Understanding the damage mechanism in these composites is very important for the development of constitutive modeling. To achieve this goal, monitoring damage initiation and accumulation *in-situ* are especially critical. In most of the previous work, the change of elastic modulus along loading direction was used to characterize the damage [1,4,5]. However, the overall anisotropic damages such as fiber-matrix debonding or shear deformation were unknown. In this study, we have pursued an *in-situ* nondestructive laser-ultrasonic technique to assess the overall anisotropic stiffness degradation under loading.

When a laser pulse is brought to sample surface, high frequency acoustic waves can be generated by thermal or ablation mechanisms depending on the incident power intensity [6,7]. The propagation of the elastic waves through anisotropic media is characterized by the well-known Christoffel equation [8]:

$$\Omega(V, \boldsymbol{n}) = \det\left|C_{ijkl}\, n_j n_l - \rho V^2 \delta_{ik}\right| = 0\,, \qquad (1)$$

where C_{ijkl} are the second-order elastic stiffness constants of the material, $\boldsymbol{n}$ is a unit vector along the bulk wave propagation direction, ρ is the density of the medium, V is the phase velocity of the elastic waves and δ_{ik} the Kroneker delta. When abbreviated subscripts are used, it can be found that $C_{IJ} = C_{ijkl}$ [8]. Based on a set of wave velocities measured along various propagation directions, the elastic constants can be deduced by fitting the experimental data to the solutions of the

Christoffel equation through nonlinear optimization procedures. Unidirectional composite can be regarded as transversely isotropic materials, thus, there are five independent elastic constants: C_{11}, C_{33}, C_{12}, C_{13} and C_{44}, while $C_{22} = C_{11}$, $C_{23} = C_{13}$, $C_{55} = C_{44}$ and $C_{66} = (C_{11} - C_{12})/2$. With the accumulation of damage in the composites, the elastic moduli will be reduced, and this will be reflected on the decreasing of the wave propagation velocities. Early study revealed that wave velocity was a good indicator of the degree of damage in CMCs [9].

When damage occurs as the result of crack initiation and growing, there is a change in the stress state of an elastic body. Accompanying this process, stress or elastic waves, often referred to as acoustic emission, are generated spontaneously and cause surface displacement which can be detected by a piezo-electric transducer attached to the sample surface [10,11]. In present study, acoustic emission (AE) events were recorded during loading/unloading of CAS/SiC composites. Information obtained from nondestructive laser-ultrasonic and mechanical testing shed new light on the damage process in fiber-reinforced unidirectional ceramic composite materials.

EXPERIMENTAL

Tensile specimens of 150 mm × 10 mm × 3 mm with continuous fibers parallel to the loading direction (the length direction of the specimen) were cut from the unidirectional CAS/SiC composite plate (provided by Corning Inc.). The specimen ends were bonded with aluminum tabs using modified epoxy (3M) to ensure even load transfer. Tensile testing was performed on an Instron 4200 machine. Axial strain was measured by a one-inch gauge length extensometer.

The ultrasonic waves was generated by a Q-switch Nd:YAG laser pulse with an operating wavelength of 1.064 μm. The pulse was delivered to the loaded sample through an optical fiber [12]. Laser scan along two principal directions of the sample was controlled by an X-Y-Z positioner with a scale of μm. Ultrasonic wave arrival at the other side of the sample was detected by two broadband piezo-electric transducers in contact with the sample. The detected signal was transferred to digital oscilloscopes. The chosen coordinates and the experimental setup are shown schematically in Fig. 1. The details of the experimental procedure will be presented elsewhere [13].

During the experiment, laser scan was performed at a pre-set stress level, and was repeated after unloading to 10 MPa. Before each scan, laser source was re-aligned to keep the laser scan along the same positions. Acoustic emission events were recorded during entire tensile test. The root-mean square average of the waveform amplitude was calculated automatically each time when the waveform was recorded.

RESULTS AND DISCUSSION

Fig. 2 shows the entire tensile stress-strain curve of the unidirectional CAS/SiC sample during loading/unloading up to 320 MPa. The acoustic emission events corresponding to loading the sample to 200 MPa is also shown. Fig. 3 displays the accumulated AE counts during entire loading/unloading process. From these figures, it is clear that in the linear region before multiple matrix cracks occur, only a few AE events were detected, and they appeared to have little effect on the macroscopic deformation behavior. With the development of damage, σ-ε curve started to deviate from linearity near the stress level of 130-150 MPa. Between the stress level of 130 MPa and 320 MPa, numerous AE events were detected and appreciable amount of inelastic deformation occurred.

During unloading from 320 MPa, a number of AE events were observed while only one or two AE signals were recorded when unloading from 200 MPa or 270 MPa. AE events during unloading are believed to be originated from interface sliding [14]; these results imply that sliding along the interface at low damage levels is not sufficient to generate AE signals, although we noticed that there was energy dissipation during unloading/reloading through frictional sliding at the fiber/matrix interfaces. As a result of energy dissipation, hysteresis loops were formed. The unloading curve from 270 MPa and 320 MPa indicates that the unloading elastic modulus does not change much, which implies that the density of matrix cracks seems to saturate near the end.

With the development of damage, the material elastic stiffnesses were degraded. This was manifest as the reduction of the ultrasonic wave velocity. The elastic stiffness constant C_{11} can be found directly from the longitudinal wave velocity at the epicenter position. In the transversely isotropic X_1X_2 plane, independent elastic constant measurements by resonant ultrasound spectroscopy technique [15] indicated that $C_{44} \approx C_{66}$, thus, C_{44} (or C_{66}) can determined by averaging the shear velocity at different scan positions in the X_1X_2 plane, because the velocity of the pure shear wave is given by $V = \sqrt{C_{44} / \rho}$.

The other unknown elastic constants C_{33} and C_{13} were determined from the wave velocity measured within the principal X_1X_3 plane. Again, the two shear modes are not clearly distinguished, thus identifying C_{33} and C_{13} was based on the longitudinal wave speeds using Eq. (1) through nonlinear curve fitting process (Peakfit software package by Jandel Scientific). The measured wave velocities in X_1X_3 plane together with the ones determined by curve fitting at four different stress levels (0, 200, 270 and 320 MPa) are plotted in Fig. 4. Significant delay of wave arrival was observed when the tensile stress was increased from 200 MPa to 270 MPa, which reflects the contribution of damage to the elastic properties. This is consistent with the plateau region shown on the σ-ε curve. Similar measurements and calculations were carried out for another sample at the stress levels of 180 and 240 MPa.

The measurements performed at 10 MPa after unloading from each successive higher stress indicate that the wave arrival velocities are changed, although not significantly when compared with those before unloading. It is noticed for most paths of reloading, AE events do not occur during reloading until near the previous peak stress level. These observations indicate that unloading/reloading does not contribute to additional damage significantly. However, after intensive damage accumulation, the AE events re-occurred at relatively lower stress level.

Elastic constants C_{11}, C_{33} and C_{44} together with the unloading elastic moduli E^* obtained from the partial unloading test are plotted in Fig. 5. C_{11}, C_{33} and E^* show the same trend of reduction, although the degree of reduction near the end of matrix crack saturation for E^* seems to be less than that of C_{11}, C_{33}.

Laser-ultrasonic measurements showed that there is overall degradation of elastic stiffness constants. The reduction of C_{11} and C_{66} in the transverse plane is believed to be associated with the damage (sliding and debonding) along interfaces, and this softening effect is still under our current investigation. The accumulation of interface damage reduces the propagation speed of ultrasound waves in the transverse plane. Fig. 6 shows the matrix cracking and damage near interface for a sample unloaded from 320 MPa. These results demonstrate that wave propagation is sensitive to the degradation of the elastic stiffness.

CONCLUSIONS

Laser-ultrasonic technique has been applied successfully to study the damage evolution in unidirectional fiber-reinforced CAS/SiC ceramic composites. Elastic constants were determined based on ultrasound wave velocity measured along various propagation directions. The results show that wave propagation is sensitive to the damage accumulation in the sample. In conjunction with AE recording, the nondestructive laser-ultrasonic method provides us valuable knowledge of the overall anisotropic damage in fiber-reinforced ceramic composites. Damage accumulation under loading is manifest as the reduction of elastic constants, the AE counts, and the σ-ε hysteresis loops. The fiber/matrix interface plays a dominant role in the overall mechanical deformation of these fiber-reinforced ceramic composites.

ACKNOWLEDGMENTS

This work was co-supported by ARPA funded UCSB-URI and the US Department of Energy, office of Basic Energy Sciences. Discussions with Dr. Y. Lu (University of Virginia), and A. G. Evans (Harvard University) are greatly appreciated.

REFERENCES

[1] D. S. Beyerle, S. M. Spearing, F. W. Zok, and A. G. Evans, "Damage and Failure in Unidirectional Ceramic-Matrix Composites", *J. Am.. Ceram. Soc.*, **75** [10] 2719-2725 (1992).

[2] C. Cady, T. J. Mackin, and A. G. Evans, "SiC/CAS: a Notch-Insensitive Ceramic-Matrix Composite", *J. Am. Ceram. Soc.*, **78** [1] 77-82 (1995).

[3] M. Y. He, B.-X. Wu, A. G. Evans, and J. W. Hutchinson, "Inelastic Strains due to Matrix Cracking in Unidirectional Fiber-Reinforced Composites", *Mech. Mater.*, **18** 213-229 (1994).

[4] M. Drissi-Habti, "Damage Development and Moduli Reduction in a Unidirectional SiC-MAS. L. Composite Tested Under Uniaxial Tensile Loading", *Script Metal. Mater.*, **33** 967-973 (1995).

[5] C. Cady, F. E. Heredia, and A. G. Evans, "In-Plane Mechanical Properties of Several Ceramic-Matrix Composites", *J. Am. Ceram. Soc.*, **78** [8] 2065-2078 (1995).

[6] S. J. Davies, C. Edwards, G. S. Taylor, and S. B. Palmer, "Laser-Generated Ultrasound: its Properties, Mechanisms and Multifarious Applications", *J. Phys. D.: Appl. Phys.*, **26** 329-348 (1993).

[7] C. B. Scruby, and L. E. Drain, *Laser Ultrasonics, Technique and Applications*, Adam Hilger, Bristol, 1990.

[8] B. A. Auld, *Acoustic Fields and Waves in Solids*, Krieger Publishing Company, Malabar, Florida, 1990.

[9] S. Baste, R. E. Guerjouma and B. Audoin, "Effect of Microcracking on the Macroscopic Behavior of Ceramic Matrix Composites: Ultrasonic Evaluation of Anisotropic Damage", *Mech. Mater.* **14** 15-31 (1992).

[10] C. B. Scruby, H. N. G. Wadley, and J. J. Hill, "Dynamic Elastic Displacements at the Surface of an Elastic Half-space due to Defect Sources", *J. Phys. D: Appl. Phys.*, **16** 1069-1083 (1983).
[11] D. G. Eitzen and H. N. G. Wadley, " Acoustic Emission: Establishing the Fundamentals", *Journal of Research of the National Bureau of Standards*, **89** 75-100 (1984).
[12] R. J. Dewhurst, A. G. Nurse, and S. B. Palmer, "High Power Optical Fibre Delivery System for the Laser Generation of Ultrasound", *Ultrasonics*, **26** 307-310 (1988).
[13] Y.-M. Liu, T. E. Mitchell, and H. N. G. Wadley, "Dynamic Elastic Observations of Damage in Fiber-Reinforced Ceramics", to be submitted to *Acta Mater.*, 1996.
[14] J.-J. Luo, S.-C. Wooh, and I. M. Daniel, "Acoustic Emission Study of Failure Mechanisms in Ceramic Matrix Composite under Longitudinal Tensile Loading", *Review of Progress in Quantitative Nondestructive Evaluation*, Vol. **13**, edited by D. O. Thompson and D. E. Chimenti, Plenum Press, New York, 1994.
[15] Y.- M. Liu, Y. He, F. Chu, T. E. Mitchell and H. N. G. Wadley, "Elastic Properties of Laminated CAS/SiC Composites Determined by Resonant Ultrasound Spectroscopy", submitted to *J. Am. Ceram. Soc.*, 1996.

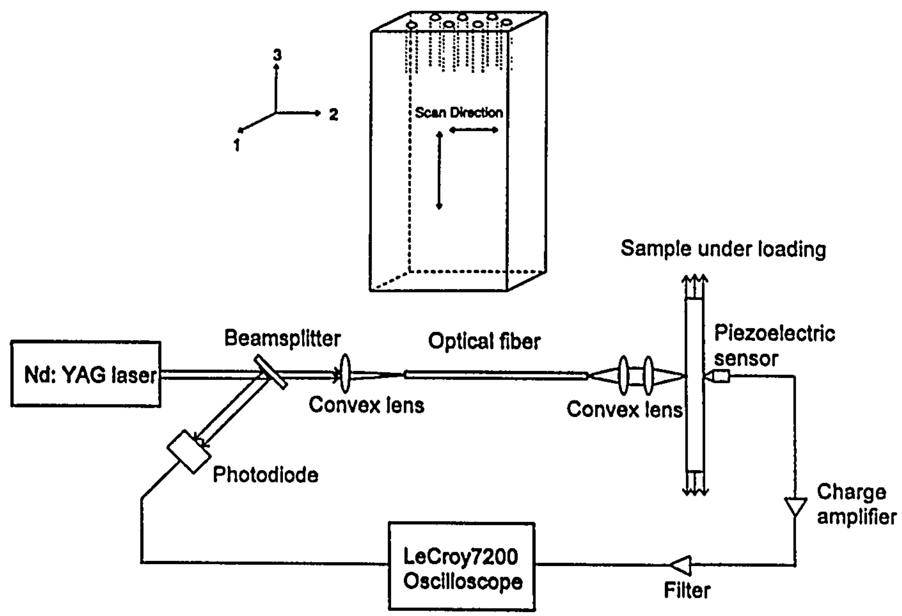
3
2
1
Scan Direction
Sample under loading
Nd: YAG laser
Beamsplitter
Optical fiber
Piezoelectric
sensor
Convex lens
Convex lens
Photodiode
Charge
amplifier
LeCroy7200
Oscilloscope
Filter

Fig. 1

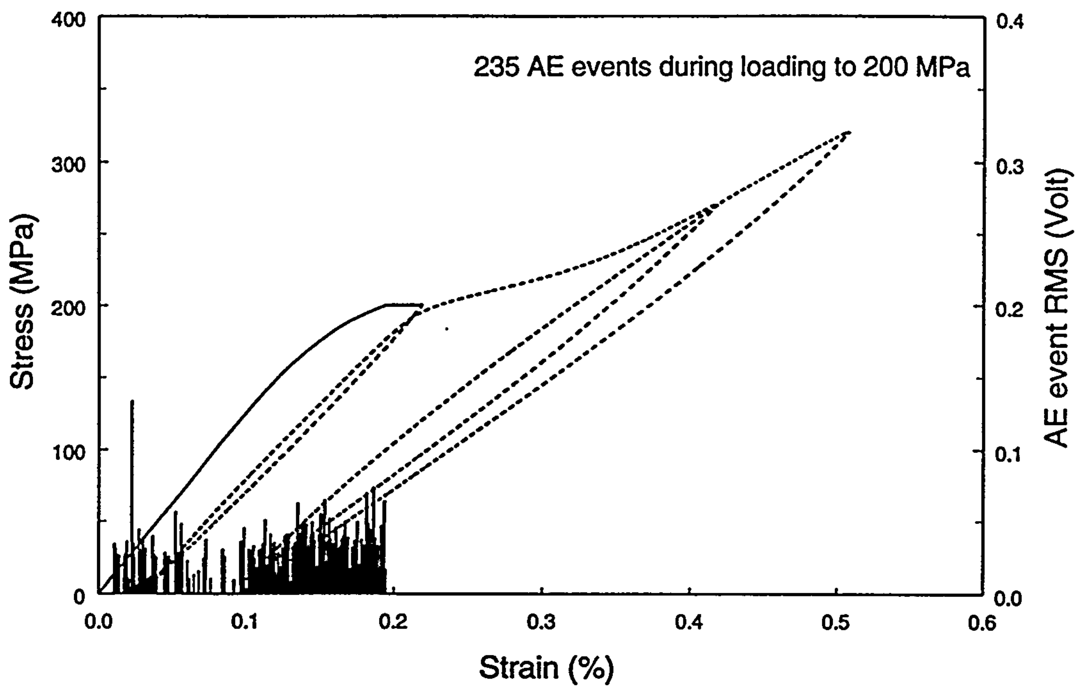

235 AE events during loading to 200 MPa
Stress (MPa)
AE event RMS (Volt)
Strain (%)
400
300
200
100
0
0.4
0.3
0.2
0.1
0.0
0.0
0.1
0.2
0.3
0.4
0.5
0.6

Fig. 2

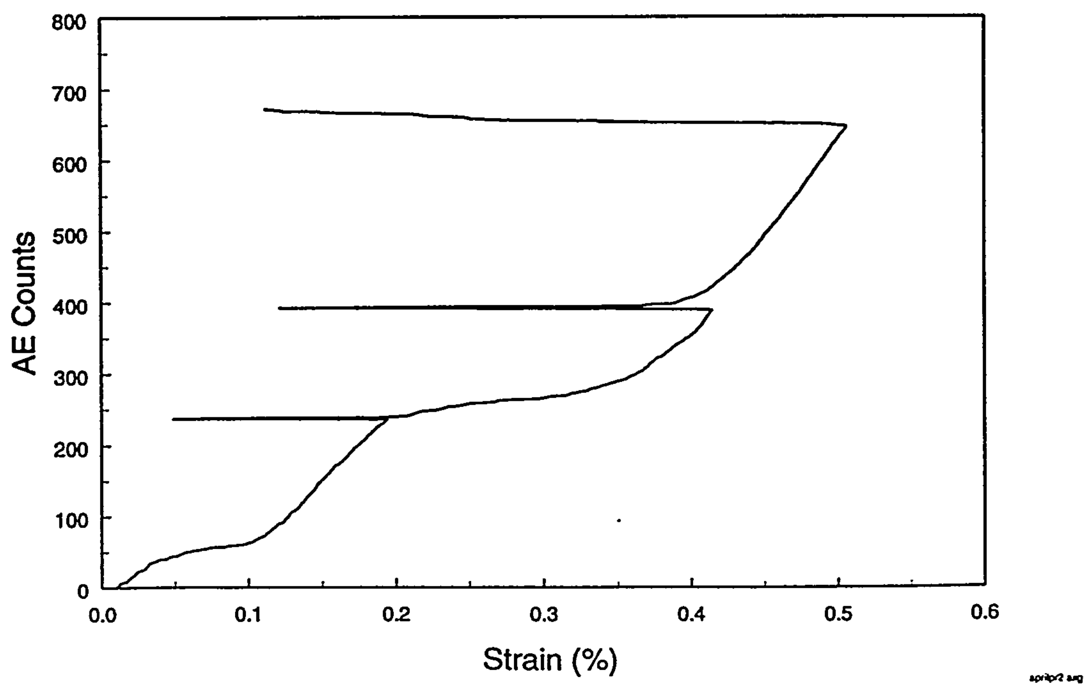

AE Counts
Strain (%)
800
700
600
500
400
300
200
100
0
0.0
0.1
0.2
0.3
0.4
0.5
0.6

Fig. 3

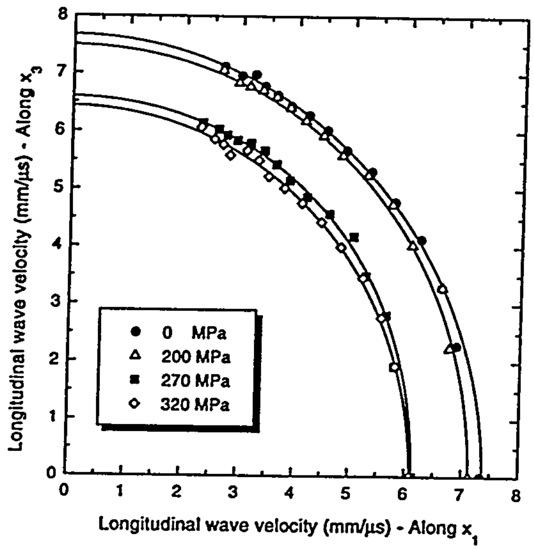

Longitudinal wave velocity (mm/µs) - Along x_3
Longitudinal wave velocity (mm/µs) - Along x_1
0 MPa
200 MPa
270 MPa
320 MPa

Fig. 4

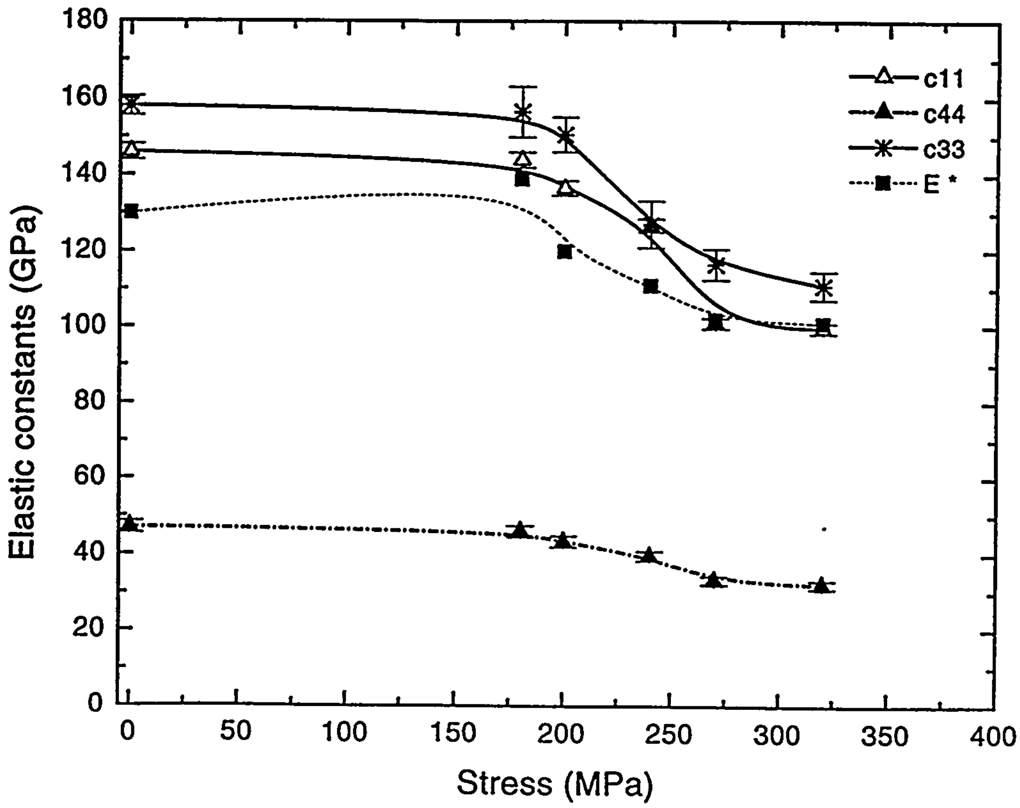

Elastic constants (GPa)
Stress (MPa)
c11
c44
c33
E *

Fig. 5

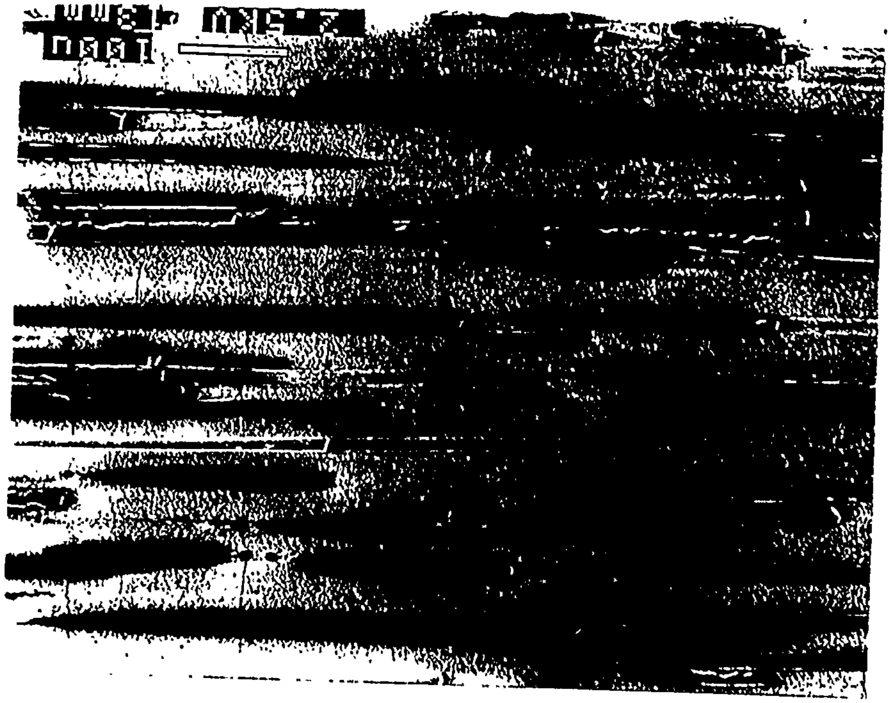

Fig. 6